IMMUNOLOGY

Induced, but not natural, regulatory T cells retain phenotype and function following exposure to inflamed synovial fibroblasts

Sujuan Yang[1,2]*, Ximei Zhang[1,3]*, Jingrong Chen[1]*, Junlong Dang[1,2], Rongzhen Liang[1], Donglan Zeng[1], Huan Zhang[1], Youqiu Xue[3], Yan Liu[1], Wenbin Wu[1], Jun Zhao[1], Julie Wang[3], Yunfeng Pan[1], Hanshi Xu[4], Bing Sun[5], Feng Huang[1], Yan Lu[1], Willa Hsueh[3], Nancy Olsen[2], Song Guo Zheng[3]†

Copyright © 2020 The Authors, some rights reserved; exclusive licensee American Association for the Advancement of Science. No claim to original U.S. Government Works. Distributed under a Creative Commons Attribution NonCommercial License 4.0 (CC BY-NC).

Aberrant number and/or dysfunction of CD4$^+$Foxp3$^+$ Regulatory T cells (T_{regs}) are associated with the pathogenesis of rheumatoid arthritis (RA). A previous study has demonstrated that thymus-derived, natural T_{regs} (nT_{regs}) prefer to accumulate in inflamed joints and transdifferentiate to T_H17 cells under the stimulation of inflamed synovial fibroblasts (SFs). In this study, we made a head-to-head comparison of both T_{reg} subsets and demonstrated that induced T_{regs} (iT_{regs}), but not nT_{regs}, retained Foxp3 expression and regulatory function on T effector cells (T_{effs}) after being primed with inflamed SFs. In addition, iT_{regs} inhibited proliferation, inflammatory cytokine production, migration, and invasion ability of collagen-induced arthritis (CIA)–SFs in vitro and in vivo. Moreover, we noted that iT_{regs} directly targeted inflamed SFs to treat autoimmune arthritis, while nT_{regs} failed to do this. Thus, manipulation of the iT_{reg} subset may have a greater potential for prevention or treatment of patients with RA.

INTRODUCTION

Rheumatoid arthritis (RA) is a chronic, progressive, and systemic autoimmune disorder characterized by primary inflammatory synovitis, subsequent articular cartilage destruction, and bone erosion. Inflamed synovial fibroblasts (SFs) are a dominant cell type involved in the pathogenesis of RA (*1*). These cells have a semitransformed, autoaggressive phenotype characterized by reduced apoptosis, production of matrix-degrading enzymes, secretion of proinflammatory cytokines and receptor activator of nuclear factor-κ B ligand (RANKL) that promote osteoclasts differentiation, and the subsequent bone destruction (*2*, *3*).

It is well recognized that CD4$^+$Foxp3$^+$ regulatory T cells (T_{regs}) play an essential role in maintaining immune homeostasis and preventing autoimmune diseases (*4*). T_{regs} abnormalities in number and/or function may contribute to many autoimmune diseases including RA (*5*). T_{regs} are heterogeneous and consist of at least two types, thymus-derived naturally occurring (nT_{regs}) and induced T_{reg} (iT_{reg}) developed in the periphery or in vitro after stimulation with interleukin-1 (IL-2) and transforming growth factor–β (TGF-β) (*6*). We and others have previously reported that both T_{reg} subsets not only share similarities but also display some differences (*7*, *8*).

Komatsu *et al.* (*9*) provided evidence that adoptively transferred nT_{reg} preferentially lost Foxp3 expression, transdifferentiated to pathogenic T helper 17 (T_H17) cells mediated by SF-derived IL-6 and accumulated in the inflamed synovium in a collagen-induced arthritis (CIA) model. These ex-Foxp3 T_H17 cells accelerated the onset and increased the severity of arthritis. Our hypothesis is that iT_{regs} have different biological characteristics following the priming with inflamed SFs, as compared to nT_{regs}. We aimed to address the hypothesis by directly comparing nT_{reg} and iT_{reg} subsets in inflammatory conditions in vitro and in the established colitis and CIA mouse models in vivo.

RESULTS

iT_{reg} subset retains Foxp3 expression and regulatory function on Teff after being primed with CIA-SFs in vitro

To determine whether iT_{regs} similarly lose Foxp3 and regulatory function as nT_{regs}, we firstly isolated inflamed SF from CIA mice (CIA-SFs, purity > 90%; fig. S1, A to D) and then cocultured nT_{reg} or iT_{reg} subsets with CIA-SFs in a cell-cell contact manner (10:1 ratio of SFs to T_{reg} subsets), as performed in Komatsu *et al.*'s study (*9*). We also performed CIA-SF identification after multiple passages. As we expected, the SFs maintained their phenotypic characteristics, such as the expression of vascular cell adhesion molecule–1 (VCAM-1), intercellular adhesion molecule–1, and fibroblast activation protein α (FAPα) (*10*, *11*). We used nT_{reg} cultured under the condition for T_H17 cell differentiation as a control. nT_{regs} and iT_{regs} cultured alone expressed a similar high level of Foxp3 and rarely IL-17A (Fig. 1A). nT_{reg} cultured alone under the stimulation of IL-6 or cocultured with inflamed SFs preferentially lost Foxp3 expression and some transdifferentiated into T_H17 cells (Fig. 1A), while iT_{reg} treated with CIA-SFs showed no substantial difference when compared to T_{regs} cultured alone. We also observed that pT_{reg} isolated from lymph node lost Foxp3 expression and transdifferentiated to T_H17 cells after being cocultured with CIA-SFs, which is similar to pT_{reg} or naïve CD4$^+$ T cells cultured under T_H17 cell differentiation (fig. S2A). When we extended the coculture time from 3 to 7 days, we observed that nT_{reg} cocultured with CIA-SFs sharply lost Foxp3 expression and increasingly transdifferentiated to T_H17 cells (fig. S2, B and C). In addition, both nT_{regs} and iT_{regs} rarely expressed various transcript factors of T effector cells (T_{effs}) which could mediate

[1]Department of Clinical Immunology, The Third Affiliated Hospital of Sun Yat-sen University, Guangzhou 510630, China. [2]Department of Medicine, The Penn State University Hershey Medical Center, Hershey, PA 17033, USA. [3]Department of Internal Medicine, The Ohio State University Wexner Medical Center, Columbus, OH 43210, USA. [4]Department of Internal Medicine, The First Affiliated Hospital of Sun Yat-sen University, Guangzhou 510080, China. [5]Department of Immunology, Institute of Biochemistry at Chinese Academy of Science, Shanghai 200031, China.
*These authors contributed equally to this work.
†Corresponding author. Email: songguozheng2013@yahoo.com

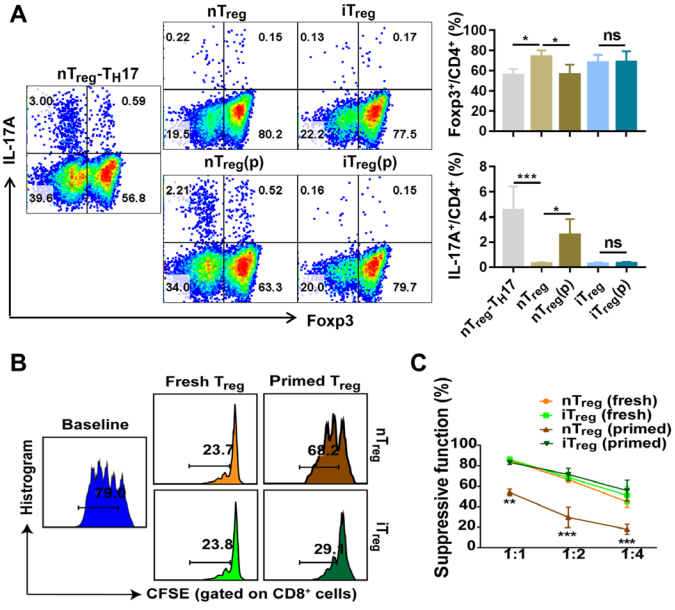

Fig. 1. iT_{reg} subset retains Foxp3 expression and regulatory function on Teff after priming with SFs isolated from CIA mice in vitro. (**A**) T_{reg} cells were cocultured with or without CIA-SFs in a cell-cell contact manner (10:1 ratio) for 3 days [namely, T_{reg} and T_{reg}(p), respectively]. nT_{reg} and iT_{reg} cultured under T_H17 differentiation condition were used as a control. The expression of IL-17A and Foxp3 on T_{reg} cells was determined by flow cytometry. (**B** and **C**) nT_{reg} and iT_{reg} cocultured with or without CIA-SFs for 3 days were collected and then cocultured with carboxyfluorescein diacetate succinimidyl ester (CFSE)–labeled Teff, respectively, at a ratio of 1:1, 1:2, and 1:4 for another 3 days; Teff cells cultured alone were used as a control(baseline). The representative images of the proliferation of $CD8^+$ T cells were showed (T_{reg}: Teff, 1:2). $n = 3$. $^*P < 0.05$, $^{**}P < 0.01$, and $^{***}P < 0.001$ by two-way analysis of variance (ANOVA). Graphs show the means ± SEM. ns, not significant.

both acute or chronic inflammatory reactions under conditions of infection or autoimmunity; however, nT_{regs}, but not iT_{regs}, began to express T-bet, RORγt, IL-23R, and Gata-3 mRNA after being exposed to inflamed SFs (fig. S3).

Foxp3 expression and stability usually reflect the functional activity of T_{regs}. To validate whether T_{regs} are still functional after being primed with CIA-SFs, we harvested the two T_{reg} subsets after being cocultured with or without CIA-SFs for 3 days and performed a standard functional assay in vitro (*12*). The results showed that both nT_{regs} and iT_{regs} without being primed with CIA-SFs had similarly excellent suppressive function against Teff proliferation (Fig. 1, B and C). After being primed with CIA-SFs, iT_{regs} maintained their suppressive function, while nT_{regs} notably lost their suppressive capacity (Fig. 1, B and C). We further analyzed whether these differences between nT_{regs} and iT_{regs} also can be seen in cells from RA patient when exposed to SFs from RA patients (RA-SFs; purity, >90%; fig. S1C). Our results suggested that both nT_{reg} and iT_{reg} from RA patient cultured alone expressed a high level of Foxp3 and low level of IL-17A (fig. S4, A and B). Similarly, after being cocultured with RA-SFs, nT_{reg} lost some Foxp3 expression and transdifferentiated to T_H17 cells, while iT_{reg} showed no notable difference from iT_{reg} cultured alone. Consistently, both nT_{reg} and iT_{reg} showed strong suppression on CD8 proliferation, RA-SFs pretreatment weakened the suppression function of nT_{reg} but not iT_{reg} on CD8 proliferation (fig. S4C). Performing t-distributed stochastic neighbor embedding (tSNE) analysis by FlowJo also indicated that nT_{reg} subset transdifferentiated more into T_H17 and T_H1 subsets after being cocultured with CIA-SFs (Fig. 2, A and B). In addition, nT_{regs} underwent a sharp reduction in the expression of CD25 under inflammatory condition (Fig. 2, A and B). The cytotoxic T lymphocyte–associated protein 4 (CTLA-4) expression was significantly lower in nT_{reg} than in iT_{reg}. iT_{regs}, but not nT_{regs}, increased CTLA-4 expression in the presence of CIA-SFs (Fig. 2, A and B). We also observed that IL-6 stimulation decreased the expression of CD39, Helios, Nrp-1, and interferon regulatory transcription factor 4 (IRF4) on nT_{reg} and had no effect on T cell immunoreceptor with Ig and ITIM domains (TIGIT), OX-40, glucocorticoid-induced TNF (tumor necrosis factor) receptor (GITR), Blimp-1, 4-1BB, inducible co-stimulator (ICOS), and CTLA-4 expression when compared to nT_{reg} cultured alone. CIA-SFs priming did not affect the expression of OX-40, Nrp-1, TIGIT, and CIA-SFs on both nT_{reg} and T_{regs} (fig. S2D). CIA-SFs priming lowered the expression of CD137 (also called 4-1BB), ICOS, Helios, CD39, CTLA-4, and IRF4 and increased the expression of GITR and Blimp-1 by nT_{reg} when compared to nT_{reg} cultured alone (Fig. 2C and fig. S2D). In contrast, CIA-SFs priming did not affect most of these markers expression on iT_{reg} while increasing CD39 and CTLA-4 expression by iT_{reg} (Fig. 2C and fig. S2D). These results further support that nT_{reg}, but not iT_{reg}, encounters a functional decline when exposed to the inflamed synovial tissues (*9*). Furthermore, under the stimulation of inflammatory microenvironment caused by CIA-SFs, iT_{reg}, but not nT_{reg}, successfully differentiates into effector T_{reg} (eT_{reg}).

iT_{reg} subset maintains regulatory function on Teff after being primed with CIA-SFs in vivo

The functional activity of T_{regs} in vitro does not necessarily reflect their functional effect on the disease in vivo. We chose a colitis model because it is a Teff-mediated disease to determine the functional activities of T_{reg} subsets in vivo (*13*). Naïve $CD4^+$ T cells (0.6 million) from $CD90.1^+$ C57BL/6 mice were injected into $Rag1^{-/-}$ mice alone or together with 0.6 million of either nT_{reg} or iT_{reg} subsets isolated or induced, respectively, from $CD90.2^+$ $Foxp3^-$green fluorescent protein (GFP) reporter mice after being primed with or without CIA-SFs on the same day. We found that the colitis model that had only received naïve $CD4^+$ T cells gradually lost weight from day 9 onward and gradually developed typical severe colitis on day 33 (Fig. 3A). Cotransfer the nT_{reg} or iT_{reg} subset markedly suppressed the appearance of colitis, indicating that both T_{reg} subsets are functional in the disease condition in vivo. Recipient mice of either nT_{reg} or iT_{reg} without priming or iT_{reg} with priming slowly gained weight and only showed slight but not notable colitis (Fig. 3A). In contrast, when nT_{regs} were primed with inflamed SFs, they no longer suppressed colitis. Nonetheless, cotransfer of the iT_{reg} subset that had been primed with inflamed SFs still potently controlled the colitis (Fig. 3A).

As expected, in this colitis model, 30% of $CD4^+CD90.1^+$ cells produced IL-17A or interferon-γ (IFN-γ) and 5% produced both IL-17A and IFN-γ in the spleen (Fig. 3, B and C). Similar results were seen in mesenteric lymph nodes (mLNs) and colonic lamina propria (cLP) (Fig. 3C). Both nT_{reg} and iT_{reg} subsets without priming potently suppressed the differentiation of naïve $CD4^+$ T cells ($CD90.1^+$) to T_H17 and T_H1 cells and inhibited the proliferation of Teff in the spleen, mLNs, and cLP (Fig. 3, B and C). After priming, nT_{regs} almost completely lost their suppressive activity, while iT_{regs} sustained this ability (Fig. 3, B and C).

To trace the fate of T_{reg} subsets in the colitis mice, we detected Foxp3 and IL-17A expression on $CD90.2^+$ T_{reg} following an in vivo

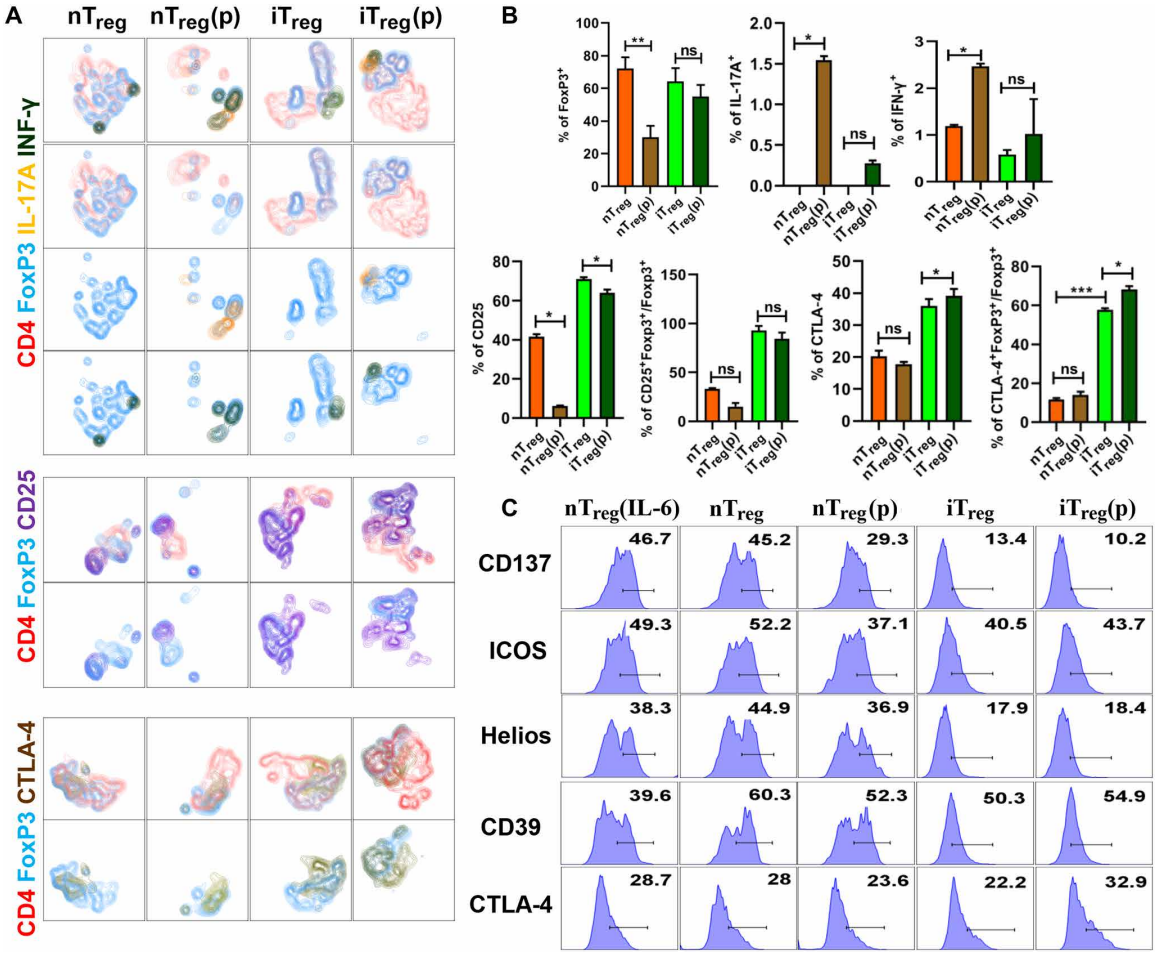

Fig. 2. iT_{reg} is more stable than nT_{reg} in the presence of CIA-SFs. (**A** and **B**) T_{regs} were cocultured with or without CIA-SFs (lower chamber) in a cell-cell contact at a ratio of 10:1 for 3 days. The expression of T_{reg} or T_H cell markers was detected using flow cytometry. The coexpression of T_{reg} markers and T_H cell markers are shown using t-distribution and Stochastic Neighbor Embedding (tSNE) plots in the left panel (A). The summary data are shown in the right panel (B). (**C**) T_{regs} were cocultured with or without CIA-SFs (lower chamber) in a ratio of 1:20 for 7 days. The expression of CD137, Helios, ICOS, CD39, and CTLA-4 by T_{regs} were analyzed by flow cytometry. $n = 3$. $^*P < 0.05$, $^{**}P < 0.01$, and $^{***}P < 0.001$ by one-way ANOVA. Graphs show the means ± SEM.

transfer. Consistent with the above results, both nT_{reg} and iT_{reg} subsets without priming mostly maintained the Foxp3 expression and resisted T_H17 transdifferentiation (Fig. 3, D and E). However, the nT_{reg} subset primed with CIA-SFs significantly lost Foxp3 expression and acquired a T_H17/T_H1 phenotype, especially in cLP, indicating some nT_{regs} have converted to inflammatory cells (Fig. 3, D and E). Conversely, iT_{regs} primed with inflamed SFs maintained Foxp3 and resisted T_H17 conversion (Fig. 3, D and E). Hematoxylin and eosin (H&E) staining showed that the colitis model developed a severe inflammatory cell infiltration, ulcers, edema, and bowel wall thickening (Fig. 3F). Both nT_{reg} and iT_{reg} subsets without priming strongly inhibited inflammatory cell infiltration and kept epithelial cells and goblet cells intact. Severe inflammatory cell infiltration and mucous membrane ulceration were observed with cotransfer of nT_{regs} that had been primed with inflamed CIA-SFs. In sharp contrast, cotransfer of iT_{regs} primed with CIA-SFs exhibited less inflamed pathology and fewer inflammatory cells (Fig. 3F). These results strongly suggest that the iT_{reg} subset has superior stability and better biological activity in down-regulating T_H17/T_H1 cells differentiation and Teff proliferation in autoimmune and inflammatory conditions, particularly following exposure to inflamed SFs.

iT_{reg}, but not nT_{reg}, maintains therapeutic effect in CIA model after being pretreated with CIA-SFs

Since we have observed that iT_{reg}, but not nT_{reg}, pretreated with CIA-SFs maintained their stability with little transdifferentiated into T_H17 cells in vitro and in colitis model, we further hypothesized that iT_{reg}, but not nT_{reg}, being pretreated with CIA-SFs in vitro retained their therapeutic effect in CIA mice. To this end, we pretreated nT_{reg} and iT_{reg} with or without CIA-SFs (SFs to T_{regs}, 1:10) for 3 days and then intravenously injected these cells (3×10^6 per mouse) into CIA mice on day 27 after immunization when the onset of clinical symptoms of arthritis was observed. We observed that both iT_{reg} and nT_{reg} treatments reduced clinical scores and inhibit bone erosion in CIA mice (Fig. 4, A and B). Mice received nT_{reg} being pretreated with CIA-SFs showed no substantial alleviation when compared to mice receiving no treatment (Fig. 4, A and B). In contrast, the transfer of iT_{reg} being pretreated with CIA-SFs remained markedly decreased the severity of arthritis, showing no notable therapeutic

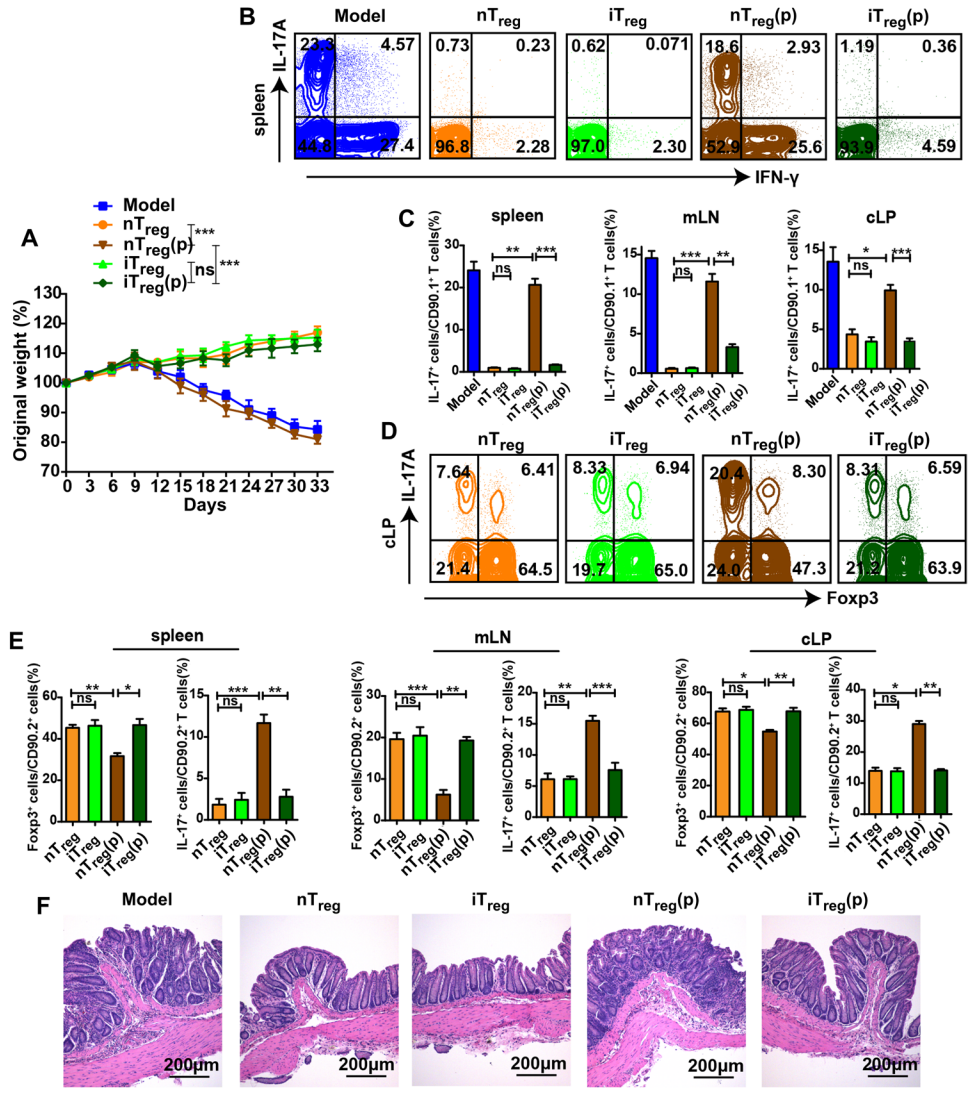

Fig. 3. iT$_{regs}$ after being primed with CIA-SFs maintain the phenotype and suppressive function on T$_{effs}$ in vivo in colitis model. Naïve CD4$^+$ T cells (0.6 million) from CD90.1$^+$ Foxp3$^-$GFP reporter C57BL/6 mice were intraperitoneally injected into Rag1$^{-/-}$ mice alone or together with 0.6 million of the two T$_{regs}$ subsets from CD90.2$^+$ Foxp3$^-$GFP reporter DBA1/J mice after being primed with or without CIA-SFs at the same day. Weights of the recipient mice were monitored per 3 days after the cell transfer. Thirty-three days later, single cells from spleen, mLNs, and cLP were harvested. (**A**) Weight change of the mice from different groups. (**B** and **C**) The proportions of Foxp3$^+$ cells and IL-17A$^+$ cells on CD90.1$^+$ cells were determined. (**D** and **E**) The proportions of Foxp3$^+$ and IL-17A$^+$ cells on CD90.2$^+$ cells were determined. (**F**) The colon was subjected to H&E staining (40×; scale bars, 200 μm) and the development of colitis was evaluated blindly by two pathologists. $n = 6$. *$P < 0.05$, **$P < 0.01$, and ***$P < 0.001$ by one-way ANOVA(C and E) and two-way ANOVA (A). Graphs show the means ± SEM.

difference to iT$_{reg}$ treatment (Fig. 4, A and B). Notably, the transfer of nT$_{reg}$ and iT$_{reg}$ increased the number of Foxp3$^+$ T$_{regs}$ while decreased the number of IFN-γ$^+$ T$_H$1 cells in the joint fluid (Fig. 4, C to F). Consistently, infusion of iT$_{regs}$ being pretreated with CIA-SFs also markedly increased the number of T$_{regs}$ while decreased the number of T$_H$1 cells in the joint fluid, whereas infusion of nT$_{reg}$ being pretreated with CIA-SFs showed no effect on the number of Foxp3$^+$ T$_{regs}$ and IFN-γ$^+$ T$_H$1 cells in the joint fluid when compared to mice with no treatment (Fig. 4, C to F). We also observed that both iT$_{reg}$ and iT$_{reg}$ being pretreated with CIA-SFs markedly lowered the expression of T$_H$17 cells in lymph node cells (Fig. 4, G and H). While nT$_{reg}$ treatment also showed a reduced on T$_H$17 cells in lymph node cells, infusion of nT$_{reg}$ being pretreated with CIA-SFs showed no effect on T$_H$17 cell expression in lymph node cell of CIA mice (Fig. 4, G and H). These results suggest that iT$_{reg}$, but not nT$_{reg}$, retained their therapeutic function in CIA mice after being primed with CIA-SFs.

iT$_{regs}$ inhibit the inflammatory activities of CIA-SFs in vitro

Previous studies have reported that proinflammatory cytokines secreted by inflamed SFs, including tumor necrosis factor–α (TNFα), IL-1β, IL-6, matrix metalloproteinase–9 (MMP9), and others, are not only triggers of chronic inflammation but also promoters of pannus formation and cartilage degradation (*14*). The tumor-like biologic behaviors of inflamed CIA-SFs including proliferation, migration, and invasion also contribute to the severity of arthritis (*15*). Although previous studies have suggested that T$_{regs}$ can directly

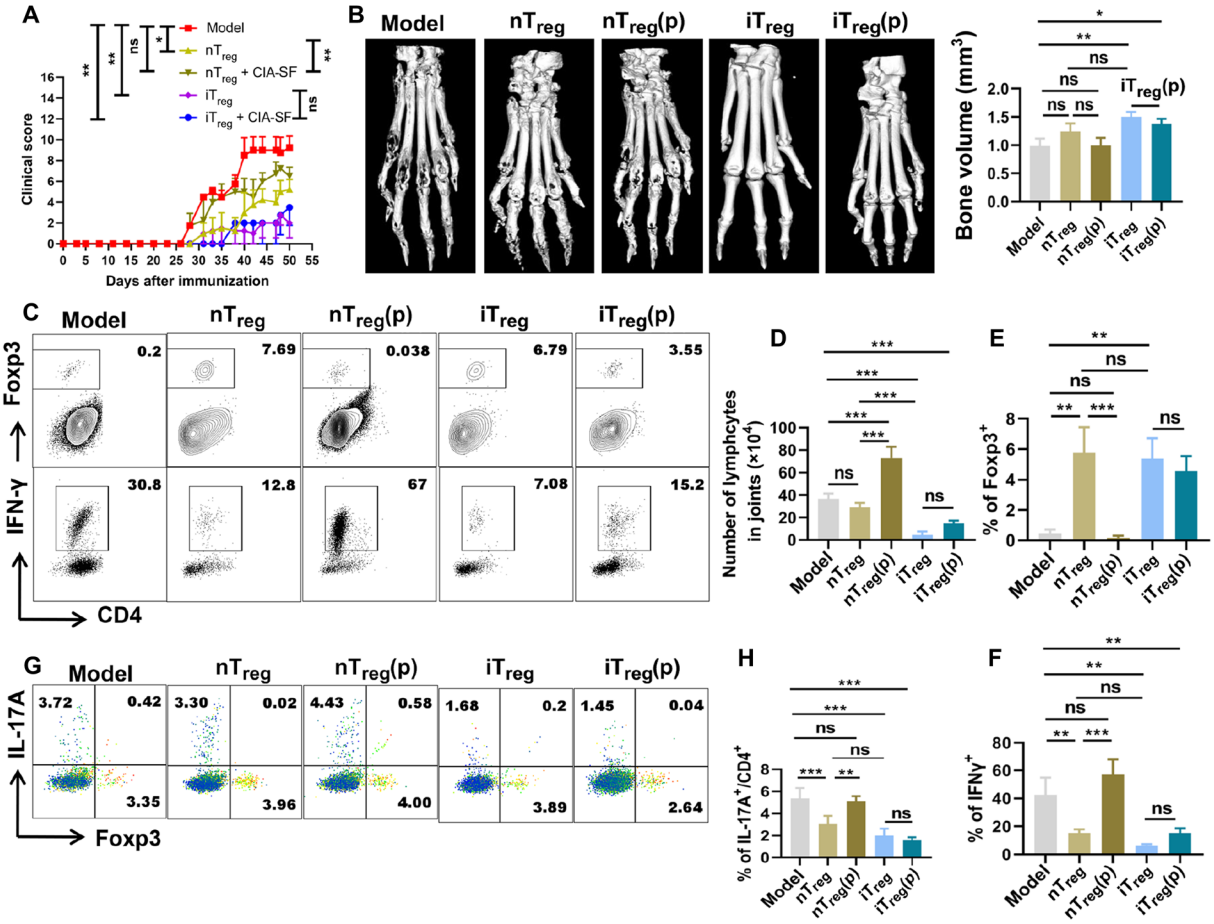

Fig. 4. iT_{reg}, but not nT_{reg}, maintains therapeutic effect in CIA model after being pretreated with CIA-SFs. CIA was induced in DBA1/J mice with CII/CFA. T_{regs} (3×10^6) after being pretreated with or without [namely, T_{reg} and T_{reg}(p) respectively]. CIA-SFs for 3 days (T_{regs} to CIA-SFs, 10:1) were adoptively transferred into the established CIA mice on day 28 after the immunization, CIA model without any treatment was set as a control. (**A**) Clinical scores were recorded every 2 to 3 days after the onset of arthritis, and mice were sacrificed on day 50 after immunization. (**B**) Representative micro–computed tomography imaging of ankle joints and bone volume of the metatarsophalangeal joints from CIA mice of different treatment. (**C** to **F**) Cells in the joint fluid were collected and stimulated with PMA and ionomycin for 1 hour and then with brefeldin A, followed by incubation for another 4 hours. The expression of Foxp3, IFN-γ, and IL-17A by these cells was analyzed by flow cytometry. (**G** and **H**) Single cells isolated from draining lymph nodes were stimulated with PMA and inomycin for 1 hour and then with brefeldin A, followed by incubation for another 4 hours. The expression of Foxp3 and IL-17A by these cells were analyzed by flow cytometry. $n = 5$. $^*P < 0.05$, $^{**}P < 0.01$, and $^{***}P < 0.001$ by one-way ANOVA (B, D to F, and H) and two-way ANOVA (A). Graphs show the means ± SEM.

target T_{effs}, B cells, macrophages, dendritic cells and osteoclast cells (*16*–*20*), their effects on the activities CIA-SFs remain elusive. To this end, we developed in vitro experiments to determine the regulatory function of T_{regs} on inflamed SFs. Our result suggested that iT_{regs}, but not nT_{regs}, significantly inhibited the migration of CIA-SFs (Fig. 5, A and B). We also observed that iT_{reg}, but not nT_{reg}, significantly inhibit the invasion of CIA-SFs in both extracellular matrix (ECM) gel and collagen gel condition (Fig. 5, A and B, and fig. S5). In addition, iT_{regs}, but not nT_{regs}, significantly inhibited the proliferation of CIA-SFs (Fig. 5C). To determine whether iT_{reg} subset inhibited cytokine expression or suppressed the expansion of inflamed SFs to indirectly reduce cytokine production, we also conducted a quantitative real-time polymerase chain reaction (PCR) assay to analyze the expression levels of transcription factors of these cytokines. As shown in Fig. 5 (D and E), mRNA levels of IL-6, IL-1β, IL-15, TNFα, MMP9, vascular endothelial growth factor (VEGF), and MMP14 were markedly lower in CIA-SFs treated with iT_{reg} when compared to those CIA-SFs treated with nT_{reg}, which suggested that iT_{reg} diminished the production of proinflammatory cytokines by CIA-SFs. Furthermore, enzyme-linked immunosorbent assay (ELISA) results also suggested that after being cocultured with iT_{regs} but not nT_{regs}, the secretion of inflammatory cytokines TNFα, IL-6, and IL-1β by CIA-SFs was almost completely abrogated (Fig. 5F).

It has been previously documented that the osteoclastogenesis in the CIA model requires the binding of RANKL to its receptor RANK (*21*). Therefore, we also sought to determine whether T_{reg} subsets affect RANKL expression on inflamed SFs. After being cocultured for 3 days, the RANKL and IL-6 expressed by CIA-SFs were detected by flow cytometry. Our result showed that iT_{regs}, but not nT_{regs}, significantly decreased the levels of IL-6 and RANKL (fig. S6A). We further performed experiment to determine on inflamed SF-mediated osteoclastogensis. As shown in fig. S7, osteoclast precursors (OCPs) were cocultured with CIA-SFs in a cell-cell contact manner in the

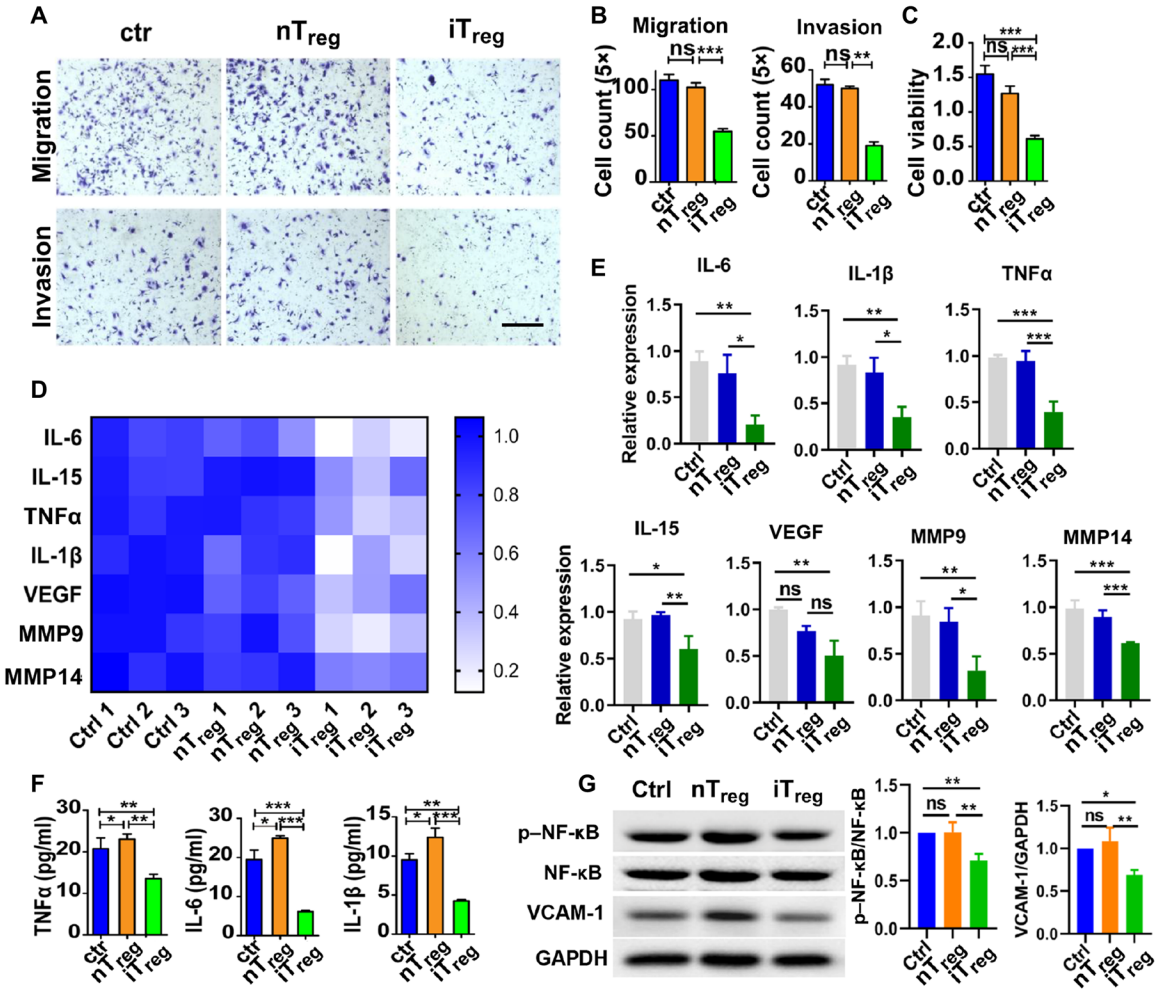

Fig. 5. iT_{reg} subset inhibits the inflammatory activities of CIA-SFs in vitro. (**A** and **B**) CIA-SFs were cocultured with the two T_{reg} subsets in 24-well transwell plate; CIA-SFs cultured alone were used as a negative control. T_{regs} were resuspended with 10% FBS and seeded in the lower chamber; CIA-SFs were resuspended with medium without FBS and seeded in the upper insert well. After 12 hours, CIA-SFs that passed through the membrane were stained with crystal violet and detected by microscope. For the invasion test, the upper chambers were coated with fresh ECM gel. The subsequent operations were conducted similarly as for migration assay. After 24 hours, CIA-SFs that passed through membrane were stained with crystal violet and detected by microscope. Scale bar, 500 μm. (**C**) We cultured CIA-SFs in the presence of iT_{regs} or nT_{regs} in 96-well plate; CIA-SFs only were set as a negative control. Three days later, the proliferation of CIA-SFs was tested with CCK-8. (**D** and **E**) CIA-SFs were cocultured with nT_{regs} or iT_{regs} in 12-well transwell system. Three days later, CIA-SFs were harvested, and qPCR analysis of relative markers was performed. GAPDH was used as an internal control in all experiments. (**F**) Cytokines including TNFα, IL-6, and IL-1β in the culture supernatants were measured by ELISA. (**G**) CIA-SFs were cultured alone or cocultured with transwell-separated T_{regs} for 3 days and then stimulated CIA-SFs from different groups with TNFα (10 ng/ml) for 30 min before collecting protein. The expression of NF-κB, phosphorylated NF-κB (p–NF-κB), and VCAM-1 by CIA-SFs was detected by Western blot, and glyceraldehyde-3-phosphate dehydrogenase (GAPDH) was used as an internal control. $n = 6$. $^{*}P < 0.05$, $^{**}P < 0.01$, and $^{***}P < 0.001$ by one-way ANOVA. Graphs show the means ± SEM.

presence of macrophage colony-stimulating factor (M-CSF), with or without T_{regs} treatment for 3 days. We observed that iT_{reg}, but not nT_{reg}, inhibit inflamed SF-mediated osteoclastogenesis. These results raise the possibility that iT_{regs} might suppress RANKL expression and then decrease osteoclastogenesis and bone erosion in autoimmune arthritis. Moreover, iT_{regs} inhibited the production of IL-6 by CIA-SFs, followed by restraining the excessive inflammatory responses in the synovial tissues.

We have observed that iT_{regs} inhibit the expression of different kinds of inflammatory factors produced by inflamed SFs, and many of these factors are now known to be under the control of the nuclear factor κB (NF-κB) transcription factors (*22*). Activated NF-κB was suggested to promote the proliferation, migration, and invasion of inflamed SFs, and the presence of activated NF-κB transcription factors has been demonstrated in animal and human inflamed SFs (*23*). Given that NF-κB signaling activation and VCAM-1 expression are associated with inflammation, cell migration, and invasion (*24*, *25*), we also evaluated whether T_{reg} subsets suppress the expression of phosphorylated NF-κB and VCAM-1in CIA-SFs. We found that iT_{regs}, but not nT_{reg}, significantly inhibited NF-κB phosphorylation and lowered VCAM-1 expression in CIA-SFs (Fig. 5G and fig. S6B).

iT_{reg} subsets exhibit a protective effect on disease and inhibit the inflammatory activities of CIA-SFs in vivo in CIA model

The superior function of iT_{regs} on CIA-SFs in vitro led us to hypothesize that iT_{reg} subset has better function in suppressing proliferation,

inflammatory cytokine production, migration, and invasion of the inflamed SFs in vivo. To address this issue, 3×10^6 nT_{reg} or iT_{reg} subsets were adoptively transferred into the established CIA model 14 days after the collagen II/ complete Freund's adjuvant (CII/CFA) immunization. After infusion for about 24 hours, nT_{reg} and iT_{reg} mainly distributed in lung, liver, spleen, kidney, lymph nodes, and some can migrate to joints of CIA mice (fig. S8, A and B). The incidence and severity of CIA were recorded every 3 days after the cell injection. We observed that infusion of nT_{regs} exhibited a diminished capacity to decrease the incidence and clinical score of CIA, while infusion of iT_{reg} markedly inhibited the incidence, delayed the onset of CIA, and decreased the clinical scores (fig. S8, C and D). We isolated CIA-SFs from CIA mice of different groups on days 45 to 60 after immunization. We found that CIA-SFs isolated from iT_{reg}-treated mice showed decreased migration, invasion, and proliferation abilities when compared to CIA-SF isolated from nT_{reg}-treated mice (fig. S8, E to G). We also observed that iT_{reg} decreased the mRNA expression level of IL-6, TNFα, and IL-1β in CIA-SFs isolated from iT_{reg}-treated CIA mice when compared with nT_{reg}-treated mice. Also, iT_{reg} also lowered the level of IL-15, VEGF, and MMP9 in CIA-SFs when compared with nT_{reg} but lack of statistically significance and inconsistent with the data in vitro. It suggests a more complicated microenvironment and context-specific iT_{regs} function in distinct immune challenge in vivo (fig. S9, A to C). As VCAM-1 and NF-κB are essential for migration and invasion of CIA-SFs (*25*), we also assessed whether T_{reg} treatment reduced the expression of phosphorylated NF-κB and VCAM-1 by CIA-SFs in vivo. In line with what we observed in vitro, iT_{regs}, but not nT_{regs}, treatment significantly inhibited NF-κB phosphorylation and VCAM-1 expression by CIA-SFs (fig. S9D). These results provide further evidence that iT_{reg} subset has a superior ability to ameliorate CIA severity by inhibiting the activities of CIA-SFs and down-regulating the proliferation, migration and invasion ability, and inflammatory cytokine production.

Inflamed SF reduced the stability of nT_{reg} and transdifferentiated nT_{reg} into T_H17 cells mainly via IL-6/IL6R signaling

We further investigated the mechanism by which inflamed SFs lowering the expression of Foxp3 and inducing the conversion T_H17 cells in nT_{regs}. We firstly compared cell-cell contact and transwell-separated coculture of T_{regs} with CIA-SFs to determine whether the effects of

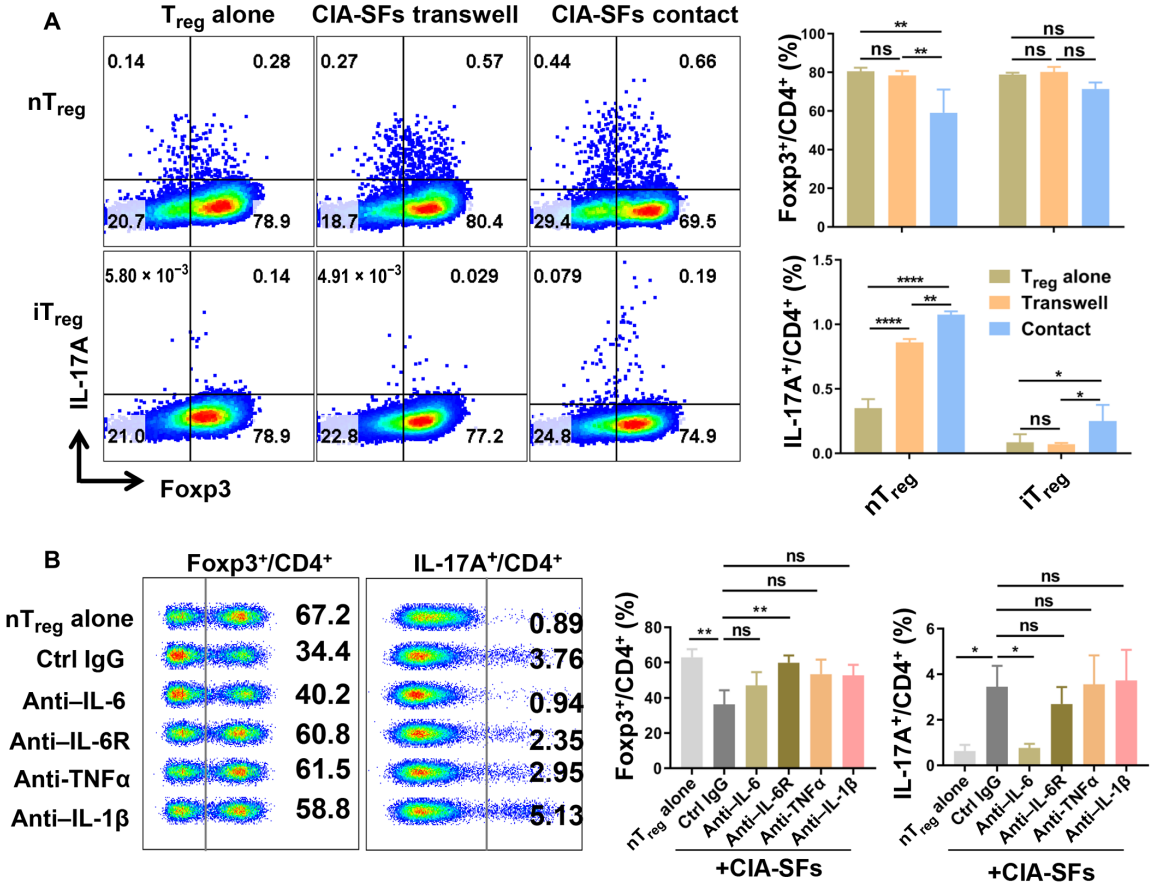

Fig. 6. Inflamed SF reduced the stability of nT_{reg} and transdifferentiated nT_{reg} into T_H17 cells mainly via IL-6/IL6R signaling. (**A**) T_{regs} were cocultured with CIA-SFs in a cell-cell contact manner or in a transwell-separated manner. T_{regs} cultured alone were set as a control. Three days later, T_{regs} were collected and stimulated with PMA and ionomycin for 1 hour and then with brefeldin A, followed by incubation for another 4 hours. The levels of Foxp3 and IL-17A expressed in these cells were analyzed by flow cytometry. (**B**) nT_{regs} were cocultured with CIA-SFs in the presence of neutralizing antibodies against IL-6, IL-6 receptor (IL-6R), IL-1β, and TNFα for 3 days. nT_{regs} cultured with or without the presence of control immunoglobulin G (IgG) were set as a control. Three days later, nT_{regs} were collected and stimulated with PMA and ionomycin for 1 hour and then with brefeldin A, followed by incubation for another 4 hours. Foxp3 and IL-17A expressed in these cells were analyzed by flow cytometry. $n = 3$. $^*P < 0.05$, $^{**}P < 0.01$, and $^{****}P < 0.0001$ by one-way ANOVA. Graphs show the means ± SEM.

CIA-SFs on T_{regs} could be attributed to soluble mediators. We observed that cell-to-cell contact contributed to Foxp3 loss while it is not essential for T_H17 cell conversion (Fig. 6A). Since we have observed that iT_{reg}, but not nT_{reg}, inhibit the production of inflammatory cytokines IL-6, IL-1β, and TNFα, which were previously reported to contribute to T_H17 differentiation (*26*), and receptors for these cytokines expressed differently on nT_{reg} and iT_{reg} (fig. S10), neutralizing antibodies against IL-6, IL-6 receptor, IL-1β, and TNFα were added to the coculture environment of nT_{reg} and CIA-SFs. Our result shows that neutralizing IL-6 almost abolished the conversion of T_H17 cells and blocking IL-6 receptor also slightly inhibit the differentiation of T_H17, whereas neither neutralization of TNFα nor neutralization of IL-1β inhibited the conversion of T_H17 cells from nT_{reg} after being priming with SFs (Fig. 6B). These results indicate that SF-derived IL-6 has a crucial role in the conversion of $Foxp3^+CD4^+$ T cells to T_H17 cells. We also observed that inhibited IL-6, IL-6 receptor, IL-1β, and TNFα all contribute to the stability of nT_{reg} (Fig. 6B). These results suggest that inflamed SF reduced the stability of nT_{reg} and converted nT_{reg} into T_H17 cells mainly via IL-6/IL6R signaling.

DISCUSSION

T_{regs} are responsible for suppressing aberrant Teff autoreactive responses and maintaining immune self-tolerance (*27*). Functional defects and declines in the proportions of T_{regs} have been linked to the pathogenesis and development of RA (*28*), while pathogenic T_H17 cells have an important role in the pathogenesis of RA by mediating osteoclastogenesis, synovial neoangiogenesis, and bone erosion. The imbalance between T_H17 and T_{reg} is strongly implicated in the onset and progression of RA (*29*).

In autoimmune arthritis, inflamed SFs constitute most of the cell population of inflamed synovial tissues and play a crucial role in the pathogenesis of RA, although T cells are also indispensable. Previous studies have shown that RA-SFs contribute to pannus formation and synovium damage by migrating and invading the cartilage and bone (*30*). Whether T_{regs} directly regulate and affect the biological behavior of inflamed SFs or not remains unknown and is a key issue.

The first study from Komatsu and colleagues revealed that half of the natural $CD25^+Foxp3^+$ T_{reg} subset lost Foxp3 expression and acquired a pathogenic T_H17 phenotype in CIA synovial fluid. IL-6 secretion by CIA-SFs in the joints drove the conversion of $CD25^+Foxp3^+$ T cells into pathogenic T_H17 cells, and in turn, IL-17 production by the formerly $Foxp3^+$ T_H17 cells induced more IL-6 from the SFs, which establishes a positive feedback loop in the arthritic joints. Moreover, these ex-Foxp3 T_H17 cells exerted more aggressive osteoclastogenic capability than T_H17 cells derived from naïve $CD4^+$ T cells because ex-Foxp3 T_H17 cells produce a considerably higher level of RANKL, which is critical in osteoclastogenesis and bone erosion (*31*). It partially explains why nT_{reg} subset is less effective in treating autoimmune arthritis (*32*). We and others provided more evidence that nT_{regs} significantly prevented but were less satisfactory in treating autoimmune arthritis because of their plasticity and conversion to T_H17, T_H1, or T follicular cells under inflammatory conditions (*33*, *34*).

The iT_{reg} subset represents another population, which mostly not only shares similarities but also displays some differences compared to nT_{reg} (*35*). Under similar inflammatory conditions, iT_{regs} were resistant to T_H17 cells conversion and maintained their phenotype and functional activities in vitro and in vivo (*8*). Both nT_{reg} and iT_{reg} subsets had a different role in suppressing osteoclastogenesis and bone protection in CIA (*20*). Recently, while high salt diet diminished the functional activities of nT_{reg} (*36*), the development and function of iT_{reg} was not comprised (*37*), demonstrating further differences in biological characteristics between nT_{reg} and iT_{reg} populations.

In this investigation, we have made a previously unidentified observation on the differences of nT_{regs} and iT_{regs} following exposure to inflamed SFs both in vitro and in vivo. While nT_{regs} primed with inflamed SFs significantly lost their Foxp3 and CD25 expression, transdifferentiated to T_H17 cells, and failed to suppress Teff proliferation in vitro and in vivo, iT_{regs} induced ex vivo highly maintained Foxp3 and CD25 expression, resisted transdifferentiating to T_H17 cells, and maintained their suppressive ability against Teff proliferation. This result further validates previous finding that $CD25^{dim}$ cells convert more into T_H17 cells (*9*). iT_{regs} display more CTLA-4 and even enhance CTLA-4 expression after being exposed to inflamed SFs; it is likely that CTLA-4 involves in the T_{reg} stability. Previous studies have demonstrated that CTLA-4 plays crucial role in the development and function of T_{regs} (*38*). In addition, our results also showed that iT_{reg}, but not nT_{reg}, retained the expression of the peculiar markers of eT_{reg}. eT_{reg} plays a vital role in the peripheral immune homeostasis. Diverse eT_{reg} subsets are activated by different antigens and cytokines. Hence, eT_{reg} gains the ability to migrate to specific tissues and exerts its particular types of function on the immune responses (*39*). Our data indicate that iT_{reg} retains the ability to transdifferentiate into eT_{reg} and maintains wholesome regulatory function under CIA-SFs priming. We also have used two animal models, colitis and CIA, to further demonstrate these differences in vivo.

Another notable observation was that the iT_{reg}, but not nT_{reg}, subset directly targeted inflamed SFs. TNFα, IL-1β, and IL-6 promote the migration and invasion of SFs, and VCAM-1 sustains the synovial inflammation and promotes adherence of peripheral blood cells to endothelial cells (*40*). RANKL is a critical determinant of osteoclastogenesis (*21*). We demonstrate that in both in vitro and in vivo experiments, iT_{regs}, but not nT_{regs}, markedly suppressed the production of inflammatory cytokines, proliferation, migration, and invasion of CIA-SFs. Moreover, iT_{regs}, but not nT_{regs}, also inhibited the activation of NF-κB in inflamed SFs. The NF-κB pathway is triggered by proinflammatory cytokines and is a participant in the pathogenic mechanisms of inflamed synovium. A previous study also demonstrated that blocking the NF-κB signaling pathways alleviates the inflammation, bone destruction, and cartilage damage in the joints (*25*).

These observations raise several possibilities to explain the differences in T_{reg} subsets under arthritic and inflamed SFs conditions. First, both T_{reg} subsets have a different response to IL-6 since we and others have previously reported that iT_{regs} have a lower level of CD126 (one of the IL-6 receptors) relative to nT_{regs} (*8*). Second, iT_{regs} but not nT_{regs} expressed undetectable SOCS1 and SOCS3 in the response to IL-6 stimulation (*41*), which promotes T_H17 cell differentiation. Third, the iT_{reg} subset that was induced with TGF-β promotes Bcl-2 expression and inhibits the apoptosis of T cells (*35*). iT_{regs} express a high level of Bcl-2, implicating that iT_{regs} are probably more resistant to apoptosis compared to nT_{reg} (*42*). Fourth, iT_{regs} may produce more IL-10 than nT_{regs} to suppress the biological activities of the inflamed SF (*32*). Fifth, iT_{reg} inhibit the production of inflammatory cytokines by inflamed SFs, including TNFα, IL-1β, and IL-6, which promote the stability of iT_{reg} in the presence of inflamed SFs.

CONCLUSION

Together, our results demonstrate that manipulation of the iT_{reg} subset may have potential promise to treat patients with RA in the future.

MATERIALS AND METHODS

Human samples

The study was approved by the medical ethics committees of Institutional Review Boards at Ohio State University and the Medical Ethics Committee of the Third Affiliated Hospital of Sun Yat-sen University. Human blood samples were obtained from the Department of Rheumatology and Immunology at the Wexner Medical center of Ohio State University and the Department of Rheumatology at the Third affiliated Hospital of Sun Yat-sen University. The synovial tissues were obtained from the National Disease Research Interchange or the Department of Rheumatology at the Third Affiliated Hospital of Sun Yat-sen University during knee arthroscopy or synovectomy. The written informed consent was obtained from the donors.

Mice

All of the C57BL/6 and DBA1/J mice from the Jackson laboratory and Nanjing Animal Institute were housed under specific pathogen–free conditions in animal rooms of Penn State Hershey Medical Center, the Ohio State University Wexner Medical Center, and the Sun Yat-sen University. All mice used in this study were 6 to 8 weeks old. All mice were treated by National Institutes of Health (NIH) guidelines for the use of experimental animals with the approval of Penn State University, Ohio State University, and Sun Yat-sen University Committees for the Use and Care of Animals.

Reagents

Dynabeads mouse/human T activator CD3/CD28 for T cell expansion and activation (anti-CD3/CD28–coated beads) were obtained from Gibco (New York, USA), and rhIL-2, rhTGFβ, recombinant mouse IL-6 (rmIL-6), and rmIL-23 were from R&D Systems (Minneapolis, MN). The carboxyfluorescein diacetate succinimidyl ester (CFSE) Cell Division Tracker Kit was purchased from BioLegend (San Diego, CA). Phorbol 12-myristate 13-acetate (PMA), ionomycin, and brefeldin A were purchased from Sigma-Aldrich. Primary antibodies against p–NF-κB, NF-κB, VCAM-1, glyceraldehyde-3-phosphate dehydrogenase (GAPDH), and rabbit anti-rat secondary antibody were purchased from Cell Signaling Technology. ELISA kits for TNFα, IL-1β, and IL-6 were from eBioscience. Incomplete Freund's adjuvant (IFA) was from Difco, MI, USA. The Cell Counting Kit-8 (CCK-8) is from Dojindo Laboratories, Kumamoto, Japan. Killed *Mycobacterium tuberculosis* strain H37Ra was purchased from Difco. ECM Gel from Engelbreth-Holm-Swarm murine sarcoma (Matrigel) and collagen from rat tail were purchased from Sigma-Aldrich. TRIzol reagent and the AMV First Strand cDNA Synthesis Kit were from Sangon Biotech Co. Ltd., Shanghai, China. Phospho–NF-κB p65 (Ser^{536}) (93H1) rabbit monoclonal antibody (mAb) (catalog no. 3033), NF-κB p65 (C22B4) rabbit mAb (catalog no. 4764), VCAM-1 (D8U5V) rabbit mAb (catalog no. 39036) VCAM-1, and GAPDH (D16H11) XP rabbit mAb were purchased from Cell Signaling Technology.

Naïve $CD4^+$ T cell isolation

Single-cell suspensions were obtained from peripheral lymph nodes and the spleen of DBA1 mice. Splenic erythrocytes were eliminated with red blood cell lysis buffer (Sigma-Aldrich). Total T cells were enriched with nylon wool. Naïve $CD4^+$ T cells that were purified from these naïve $CD4^+$ T cells were purified from these T cells via magnetic cell sorting by auto magnetic cell sorter (MACS) (Miltenyi Biotec, Germany). In brief, total cells labeled with biotin anti-CD8, CD25, B220, CD11b, CD11C, and CD49b antibodies and anti-biotin microbeads were subjected to a depletion followed by a positive selection with CD62L microbeads by auto MACS. The purity of naïve $CD4^+$ T cells were determined as $CD4^+CD25^+CD62L^+$ with flow cytometry, and the purity of >95% naïve $CD4^+$ T cells was used to induce iT_{reg}. Human naïve $CD4^+$ T cells ($CD4^+CD25^-CD45RA^+$) were isolated from human peripheral blood mononuclear cells (PBMCs) via fluorescence-activated cell sorting; the purity was >99%.

iT_{regs} induction in vitro from naïve $CD4^+$ T cells

For mouse iT_{reg} induction, the naïve $CD4^+$ T cells were cultured in the presence of anti-CD3/CD28–coated beads (cells to beads at a 1:5 ratio), recombinant human IL-2 (rhIL-2; 50 U/ml), and recombinant human TGF-β (rhTGF-β; 2 ng/ml) in 48-well plates for 3 days to induce iT_{regs}. Foxp3 expression was detected by flow cytometry about 60 to 75%. For human iT_{reg} induction, human naïve $CD4^+$ T cells were cultured in the presence of anti-CD3/CD28–coated beads (cells to beads at 1:5 ratio), rhIL-2 (50 U/ml), and rhTGF-β (5 ng/ml) in 48-well plates for 3 days. Foxp3 expression was detected by flow cytometry about 70 to 80%.

nT_{regs} and pT_{regs} isolation

Mouse $CD4^+CD25^+$ cells were sorted from the thymus of DBA1/J mice (nT_{regs}) or peripheral lymph node cells (pT_{regs}) with a purity of >95%. Around 75% $CD4^+CD25^+$ cells expressed Foxp3 as detected by flow cytometry. $CD4^+CD25^+CD127^{low}$ (purity of >99%) cells sorted from human PBMCs were used as human nT_{regs}. Foxp3 expression was detected by flow cytometry about 75 to 85%. Fresh mouse nT_{reg} and pT_{reg} were activated with anti-CD3/CD28–coated beads (1:5 to cells) in the presence of rhIL-2 (50 U/ml) for 3 days before cocultured with inflamed SFs when iT_{reg} is under induction. Fresh human nT_{regs} were amplified with anti-CD3/CD28–coated beads (1:3 to cells) in the presence of rhIL-2 (300 U/ml).

T_{regs} suppressive function in vitro

Lymphocytes were harvested, and T_{effs} from lymphocytes were enriched by nylon column and subsequently labeled with 1 μM CFSE (CellTrace CFSE Cell Proliferation Kit, Thermo Fisher Scientific). T_{effs} (0.3 million per well) were seeded in a 96-well plate, and allophycocyanins (APCs) irradiated with 30 gray (0.3 million per well) were added in the culture medium simultaneously. iT_{regs} or nT_{regs} primed with or without CIA-SFs for 3 days were added to some wells at various ratios to T_{effs}, as indicated in individual experiments. After 72-hour incubation, the proliferation of $CD8^+$ T cells was determined by flow cytometry as previously reported (*10*).

T_H17 cell differentiation

Naïve $CD4^+$ T cells were activated with anti-CD3/CD28 beads (T_{regs}: beads, 1:3) in the presence of rmIL-1β (10 ng/ml), rmIL-6 (100 ng/ml), rmIL-23 (50 ng/ml), rhTGF-β (10 ng/ml), anti–IFN-γ (5 μg/ml), and anti–IL-4 (5 μg/ml) for 3 days.

T_{regs} coculture with inflamed SFs

Inflamed SFs were cultured and activated with TNFα (10 ng/ml) stimulation for 24 hours before coculture. For a cell-to-cell contact

coculture, iT_{regs} or nT_{regs} (T_{regs}: SFs, 10:1) were added to the activated inflamed SFs directly and cocultured in the presence of anti-CD3/CD28–coated.

beads (T_{regs}: beads, 1:3) for 3 days. For transwell assays, T_{regs} were cultured in the insert well of a 24-well transwell plate (0.4-μm pore, Corning) in the presence of anti-CD3/CD28–coated beads (T_{regs}: beads, 1:3) and while SFs were cultured in the lower chamber separately to coculture for 3 days. nT_{regs}/pT_{regs} cultured under T_H17-polarizing condition (the same condition for T_H17 cell differentiated from naïve $CD4^+$ T cells) or stimulated with exogenous rmIL-6 (100 ng/ml) for 3 days were set up as a positive control. Foxp3 and IL-17A expression in T_{reg} subsets were determined by flow cytometry. For in vivo transfer, T_{regs} after being cocultured with or without CIA-SFs for 3 days were labeled with biotin anti-CD4 antibody and anti-biotin microbeads and then subjected to a positive selection by auto MACS to acquire $CD4^+$ T cells. These $CD4^+$ T cells were used as T_{regs} for transfer.

Inflamed SF-mediated osteoclastogenesis

Bone marrow cells from DBA1/J mice were labeled with Biotin anti-CD11b antibody and anti-microbeads followed by a positive selection by auto MACS to acquired CD11b + cells (purity > 95%). Then, $CD11b^+$ cells were suspended and cultured in 24 well (1×10^6 cells per well) in α-minimum essential medium culture medium [containing 10% fetal bovine serum (FBS)] in the presence of mouse M-CSF (50 ng/ml) for 3 days, and the adherent cells were used as OCPs. CIA-SFs were added directly to OCPs and then cocultured for 3 days to induce the differentiation of osteoclast. T_{regs} were seeded in the insert well in the presence of anti-CD3/CD28–coated beads (1:3 to cells) and also added to coculture with OCPs separately. OCPs cultured in the presence of mouse RANKL (50 ng/ml) and mouse M-CSF (50 ng/ml) or cocultured with CIA-SFs only for 3 days were set as a control. To evaluate osteoclast formation, cells were stained with tartrate-resistant acid phosphatase (TRAP) (Sigma-Aldrich) according to the manufacturer's instructions, and $TRAP^+$ cells were analyzed by microscopy.

Flow cytometry

The following monoclonal antibodies conjugated with fluorescein isothiocyanate, phycoerythrin, PerCP-Cy5.5, APC, or Alexa Fluor 647 were purchased from BioLegend: anti-mouse CD4 (GK1.5), CD25 (3C7), CD62L (MEL-14), PD-1 (29F.1A12), IFN-γ (XMG1.2), IL-17A (TC11-18H10.1), CD11b (M1/70), CD90.2(Thy1), CD39 (Duha59), ICOS (C398.4), OX-40 (OX-86), GITR (YGTTR/65), RANKL (IK22/5), Blimp1(5E7), TIGIT (1G9), IRF4 (IRF4.3E4), CD137 (also called 4-1BB, 17B5), Helios (22F6), NRP-1 (3E12), CTLA-4 (UC10-4B9), IFN-γ (4S.B3), IL-17A (BL168), anti-human CD11b (M1/70), Thy1 (5E10), CD4 (A161A1), CD25 (BC96), CD127 (A019D5), and Foxp3 (206D). For cell surface antigen staining, related antibodies for different antigens were diluted with phosphate-buffered saline (PBS) at 1:200, and cells were resuspended in 200-μl dilution and stained for 15 min in the dark at 4°C. The cells were washed with PBS twice and then resuspended with 500 μl of PBS followed by detecting the expression of related markers by flow cytometry immediately. For intranuclear Foxp3 staining, eBioscience Foxp3/Transcription Factor Staining Buffer Set (eBioscience) was used, and the staining was performed as described in the protocol provided with the kit. For intracellular cytokine staining, cells were stimulated with PMA (0.05 μg/ml) and ionomycin (0.5 μg/ml) (Sigma-Aldrich) for 1 hour and then with brefeldin A (10 μg/ml), followed by incubating these cells for another 4 hours at 37°C in a humidified incubator with 5% CO_2. After stimulation, first, cell surface antigen staining was performed, and the cells were fixed with fixation buffer (BioLegend) for 30 min at room temperature in the dark followed by permeabilization with 1× Intracellular Staining Perm Wash Buffer (BioLegend) for 15 min. The fixed/permeabilized cells were resuspended with 200 μl dilution in which monoclonal antibodies to cytokines were diluted at 1:100 in 1× Intracellular Staining Perm Wash Buffer (BioLegend) and stained overnight. For intranuclear and intracellular staining together, we followed the protocol for intranuclear staining. After staining, cells were washed with PBS for at least twice, resuspended in 500-μl PBS, and analyzed by flow cytometry.

Proliferation assay

CIA-SFs were cocultured with or without iT_{regs} or nT_{regs} sorted as described above (ratio 1:10) in a 96-well plate for 3 days. To detect the cell viability of CIA-SFs after being cocultured with the two T_{reg} subsets, CCK-8 (20 μl) was added to each well of the plate, and the cells were incubated at 37°C in 5% CO_2 incubator for 2 hours. We measured the absorbance at 450 nm with a microplate reader.

Migration and invasion assay

In case cell-cell contact is not necessary for the effect between T_{reg} subsets and CIA-SFs, they were cocultured in 24-well transwell plate (*9*). T_{regs} (2.5×10^5) were seeded in the lower chamber, which was filled with Dulbecco's modified Eagle's medium (DMEM) containing with 10% FBS, and then CIA-SFs (2.5×10^4) were cultured in the upper wells with DMEM without FBS. After 12 hours, CIA-SFs that passed through the membrane were fixed with 4% methanol and stained with crystal violet solution for 10 min (*43*). Photomicrographs of five random fields were obtained, and the numbers of CIA-SFs were counted. Previous study has demonstrated that RA-SF is one of the key players in invading and degrading cartilage without additional stimuli by matrix degradation. CIA-SFs' invasiveness was determined using ECM gel or collagen gel invasion (1 mg/ml, 100 μl per well) (*13*). The upper side of the chambers was coated with fresh Matrigel. T_{regs} (1×10^6) were seeded in the lower chamber, which was filled with DMEM containing 10% FBS as described above, and then CIA-SFs (1×10^5) were cultured in the upper wells with DMEM without FBS for 24 hours. CIA-SFs that passed through the Matrigel membrane were fixed and counted in the microscope as described above.

T_{regs} tracking in CIA mice

To investigate whether transferred T_{regs} can migrate into the joints of CIA mice, 3×10^6 of T_{regs} were fluorescently labeled with the Cell Tracker Red CMTPX dye (Thermo Fisher Scientific) and adoptively infused into CIA mice 14 days after immunization. Twenty-four hours later, different tissues including the heart, lung, liver, spleen, lymph node, kidney, and joint from CIA mice were collected and immediately imaged by an IVIS imaging system to determine the distribution of T_{regs}.

Induction and assessment of arthritis

CIA was induced in DBA1/J mice through intradermal injection of 100 μl of emulsion of bovine collagen II (2 mg/ml) and Complete Freund's Adjuvant containing inactivated *M. tuberculosis* (4 mg/ml) [at 1:1 (v/v) ratio]. A second immunization with 100 μl of IFA was given on day 14 after the first CII/CFA immunization.

For assessment of arthritis, clinical signs of the mice were assessed for every 3 days as follows: 0, normal joints; 0.5, swelling of one or more digits; 1, erythema and mild swelling of the ankle joint; 2, mild erythema and mild swelling involving the entire paw; 3, erythema and moderate swelling involving the entire paw; and 4, erythema and severe swelling involving the entire paw. The scores for four limbs were added together, and the maximal score for each mouse is 16. For the prophylactic function of T_{reg} in CIA model, 3×10^6 nT_{regs} or iT_{regs} were intravenously transferred to DBA/1J mice on day 14 after the first CII/CFA immunization. For the therapeutic function of T_{reg} in CIA model, 3×10^6 $CD4^+$ T_{regs} with or without being primed with CIA-SFs for 3 days were transferred to DBA/1J after the onset of arthritis was observed, around 30 days after the first CII/CFA immunization.

Induction and assessment of colitis

Naïve $CD4^+$ T cells (0.6 million) were isolated from $CD90.1^+$ $Foxp3^-$GFP reporter DBA1/J mice (wild type) and intraperitoneally injected into $Rag1^{-/-}$ mice alone or together with 0.6×10^6 $CD4^+$ T_{regs} with or without being primed with CIA-SFs for 3 days. The weights of all the $Rag1^{-/-}$ mice were monitored every day. Forty-five days after the transfer, the cells from the spleen, MLNs, and cLP were harvested from the recipient mice and were stimulated with PMA (50 ng/ml) and ionomycin (500 ng/ml). Production of IL-17A and IFN-γ by the $CD4^+$ T cells derived from $CD90.1^+$ mice was determined by flow cytometry.

Isolation of inflamed synovial tissues

For CIA-SFs isolation, CIA mice immunized for about 45 to 60 days were euthanized by cervical dislocation before dissection of inflamed joints. The four limbs of CIA mice were dissected at the joints, respectively. The skin, nail, muscle, and tendon on the specimens were removed as thoroughly as possible. We opened up the joint spaces of paws and ankles and exposed the synovial tissues in the digestive fluid with collagenase type IV (1 mg/ml), followed by strongly shaking for 1 hour at 37°C in the shaker. The SFs in the media were centrifuged at 1400 rpm for 4 min, and the cell pellet was resuspended in 10 ml of fresh media with 20% FBS. The SFs were subcultured at 90% confluence before characterization at passage four. When CIA-SFs were cultured during the passages 4 to 7 (three- to fivefold expansion), CIA-SFs were labeled with anti-mouse CD90.2-biotin antibody and anti-biotin microbeads followed by a positive selection with auto MACS. The purity of CIA-SFs was determined as $Thy1^+CD11b^-$ by flow cytometry as previously reported (purity of >90%) (*9*).

For RA-SFs isolation, the synovial tissue biopsies from RA patients were finely minced into small pieces and transferred to a tissue culture flask in DMEM (Hyclone Laboratories) supplemented with 20% FBS (Gibco), penicillin (100 U/ml; Gibco), and streptomycin (100 μg/ml; Gibco) in a humidified incubator at 37°C in 5% CO_2. RA-SFs were labeled with anti-human Thy1-biotin antibody and anti-biotin microbeads followed by a positive selection with auto MACS. The purity of CIA-SFs was determined as $Thy1^+CD11b^-$ by flow cytometry (purity of >90%).

Histopathology

For knee joints in CIA, both hind limbs from the CIA mice were dissected and incubated in 10% buffered formalin. Then, the specimens were sectioned and stained with H&E. Two pathologists blindly evaluated the global histological changes according to the proliferation of SFs, the infiltration of inflammatory cells, and the thickness and erosions of joint bone and cartilage. For colon in the colitis mice, we cut the 1-mm distal colon incubated in 10% buffered formalin and subsequently trimmed so as to render a transverse section. Subsequently, the specimens were stained with H&E. Two pathologists blindly evaluated the global histological changes according to the inflammatory cell infiltration, edema, ulcer, the intact of the epithelial cells, and goblet cells.

Enzyme-linked immunosorbent assay

The supernatants from coculture medium were subjected to ELISA for measurement of TNFα, IL-6, and IL-1β.

Western blot analysis

The collected CIA-SFs were lysed in the radioimmunoprecipitation assay lysis buffer. We detected the total protein concentration with the bicinchoninic acid protein assay and separated the proteins by using sodium dodecyl sulfate-polyacrylamide gel electrophoresis, and then the membranes were blocked with 5% skim milk for 2 hours at room temperature. The membranes were incubated in antibodies against GAPDH (1:1000), phospho–NF-κB p65 (Ser^{536}) (p–NF-κB, 1:1000) (Cell Signaling Technology, catalog no. 3033), NF-κB p65 (C22B4) rabbit mAb (Cell Signaling Technology, catalog no. 4764) p–NF-κB (1:1000), NF-κB (1:1000), and VCAM-1 (1:1000) overnight at 4°C. The next day, we washed the membranes three times to remove the redundant antibodies and incubated the membranes in horseradish peroxidase–conjugated anti-rabbit secondary antibody (1:1000) for 2 hours at room temperature. For equal loading test, the blotted membranes were stripped and reprobed with primary and secondary antibodies. The autoradiographic films were scanned and quantitated using Quantity One software (Bio-Rad, Hercules, CA).

Quantitative real-time PCR

RNA was harvested from CIA-SFs or T_{regs} using TRIzol reagent according to the manufacturer's protocol. RNA quantity and purity were confirmed with a Nanodrop spectrophotometer (Thermo Fisher Scientific). Complementary DNA (cDNA) was synthesized using the High-Capacity cDNA Reverse Transcription Kit (Applied Biosystems by Life Technologies). PCR reactions were run using the QuantStudioTM 12 K Flex real time PCR system v1.2.2 (Life Technologies TM) with SYBR Green. The following murine primers were used: IL23R (forward: 5′-GGTCCAAGCTGTCAATTCCCTAGGC-3′; reverse: 5′-AGCCCTGGAAATGATGGACGCA-3′), T-bet (forward: 5′-GTCTGGGAAGCTGAGAGTCG-3′; reverse: 5′-GAAGGACAGGAATGGAACA-3′), RORγt (forward: 5′-CATCGACAAGGCCTCCTAGC-3′; reverse: 5′-TTCCACATGTTGGCTGCACA-3′), Gata-3 (forward: 5′-AGGGACATCCTGCGCGAACTGT-3′; reverse: 5′-CATCTTCCGGTTTCGGGTCTGG-3′), IL-6 (forward: 5′-CACAAGTCCGGAGAGGAGAC-3′; reverse: 5′-CAGAATTGCCATTGCACAAC-3′), TNFα (forward: 5′-TTATCTCTCAGCTCCACGCC-3′; reverse: 5′-TGCGCACTGAAAGCATGATC-3′), MMP9 (forward: 5′-GTATGGTCGTGGCTCTAAGC-3′; reverse: 5′-AAAACCCTCTTGGTCTGCGG-3′), IL-1β (forward: 5′-TTCAGGCAGGCAGTATCACTC-3′; reverse: 5′-CCACGGGAAAGACACAGGTAG-3′), IL-15 (forward: 5′-CATATGGAATCCAACTGGA TAGATGTAAGATA-3′; reverse: 5′-CATATGCTCGAGGGACGTGTTGATGAACAT-3′),

VEGF (forward: 5′-ACTGGACCCTGGCTTTACTGCT-3′; reverse: 5′-TGATCCGCATGATCTGCATGGTG-3′), and MMP14 (forward: 5′-GTGCCCTAGGCCTACATCCG-3′; reverse: 5′-TTGGGTATCCATCCATCACT-3′).

Statistical analysis

The data were expressed as means ± SEM and analyzed using GraphPad Prism (GraphPad Software, San Diego, CA, USA). Statistical analysis and comparisons were performed using one-way analysis of variance (ANOVA), and two groups with different conditions comparisons were performed using two-way ANOVA. $P < 0.05$ is considered as statistically significant.

SUPPLEMENTARY MATERIALS

Supplementary material for this article is available at http://advances.sciencemag.org/cgi/content/full/6/44/eabb0606/DC1

View/request a protocol for this paper from *Bio-protocol*.

REFERENCES AND NOTES

1. Y. Zou, S. Xu, Y. Xiao, Q. Qiu, M. Shi, J. Wang, L. Liang, Z. Zhan, X. Yang, N. Olsen, S. G. Zheng, H. Xu, Long noncoding RNA LERFS negatively regulates rheumatoid synovial aggression and proliferation. *J. Clin. Invest.* **128**, 4510–4524 (2018).
2. S. Hawtree, M. Muthana, A. G. Wilson, The role of histone deacetylases in rheumatoid arthritis fibroblast-like synoviocytes. *Biochem. Soc. Trans.* **41**, 783–788 (2013).
3. W.-X. Peng, S.-L. Zhu, B.-Y. Zhang, Y.-M. Shi, X.-X. Feng, F. Liu, J.-L. Huang, S. G. Zheng, Smoothened regulates migration of fibroblast-like synoviocytes in rheumatoid arthritis *via* activation of Rho GTPase signaling. *Front. Immunol.* **8**, 159 (2017).
4. J. M. R. van Amelsfort, K. M. G. Jacobs, J. W. J. Bijlsma, F. P. J. G. Lafeber, L. S. Taams, CD4+CD25+ regulatory T cells in rheumatoid arthritis: Differences in the presence, phenotype, and function between peripheral blood and synovial fluid. *Arthritis Rheum.* **50**, 2775–2785 (2004).
5. M. Yang, Y. Liu, B. Mo, Y. Xue, C. Ye, Y. Jiang, X. Bi, M. Liu, Y. Wu, J. Wang, N. Olsen, Y. Pan, S. G. Zheng, Helios but not CD226, TIGIT and Foxp3 is a potential marker for $CD4^+$ Treg cells in patients with rheumatoid arthritis. *Cell. Physiol. Biochem.* **52**, 1178–1192 (2019).
6. X. Lin, M. Chen, Y. Liu, Z. Guo, X. He, D. Brand, S. G. Zheng, Advances in distinguishing natural from induced $Foxp3^+$ regulatory T cells. *Int. J. Clin. Exp. Pathol.* **6**, 116–123 (2013).
7. E. N. Huter, G. H. Stummvoll, R. J. DiPaolo, D. D. Glass, E. M. Shevach, Cutting edge: Antigen-specific TGFβ-induced regulatory T cells suppress Th17-mediated autoimmune disease. *J. Immunol.* **181**, 8209–8213 (2008).
8. S. G. Zheng, J. Wang, D. A. Horwitz, Cutting edge: $Foxp3^+CD4^+CD25^+$ regulatory T cells induced by IL-2 and TGF-β are resistant to Th17 conversion by IL-6. *J. Immunol.* **180**, 7112–7116 (2008).
9. N. Komatsu, K. Okamoto, S. Sawa, T. Nakashima, M. Oh-hora, T. Kodama, S. Tanaka, J. A. Bluestone, H. Takayanagi, Pathogenic conversion of $Foxp3^+$ T cells into T_H17 cells in autoimmune arthritis. *Nat. Med.* **20**, 62–68 (2014).
10. M. Armaka, V. Gkretsi, D. Kontoyiannis, G. Kollias, A standardized protocol for the isolation and culture of normal and arthritogenic murine synovial fibroblasts. *Protoc. Exch.* 10.1038/nprot.2009.102 , (2009).
11. A. P. Croft, J. Campos, K. Jansen, J. D. Turner, J. Marshall, M. Attar, L. Savary, C. Wehmeyer, A. J. Naylor, S. Kemble, J. Begum, K. Dürholz, H. Perlman, F. Barone, H. M. Mc Gettrick, D. T. Fearon, K. Wei, S. Raychaudhuri, I. Korsunsky, M. B. Brenner, M. Coles, S. N. Sansom, A. Filer, C. D. Buckley, Distinct fibroblast subsets drive inflammation and damage in arthritis. *Nature* **570**, 246–251 (2019).
12. S. Yang, C. Xie, Y. Chen, J. Wang, X. Chen, Z. Lu, R. R. June, S. G. Zheng, Differential roles of TNFα-TNFR1 and TNFα-TNFR2 in the differentiation and function of $CD4^+Foxp3^+$ induced Treg cells in vitro and in vivo periphery in autoimmune diseases. *Cell Death Dis.* **10**, 27 (2019).
13. W. Chen, Z. Xu, Y. Zheng, J. Wang, W. Qian, N. Olsen, D. Brand, J. Lin, S. G. Zheng, A protocol to develop T helper and Treg cells *in vivo*. *Cell Mol. Immunol.* **14**, 1013–1016 (2017).
14. S. Mateen, A. Zafar, S. Moin, A. Q. Khan, S. Zubair, Understanding the role of cytokines in the pathogenesis of rheumatoid arthritis. *Clin. Chim. Acta.* **455**, 161–171 (2016).
15. R. Xing, Y. Jin, L. Sun, L. Yang, C. Li, Z. Li, X. Liu, J. Zhao, Interleukin-21 induces migration and invasion of fibroblast-like synoviocytes from patients with rheumatoid arthritis. *Clin. Exp. Immunol.* **184**, 147–158 (2016).
16. D.-M. Zhao, A. M. Thornton, R. J. DiPaolo, E. M. Shevach, Activated $CD4^+CD25^+$ T cells selectively kill B lymphocytes. *Blood* **107**, 3925–3932 (2006).
17. Q. Ma, J. Liu, G. Wu, M. Teng, S. Wang, M. Cui, Y. Li, Co-expression of LAG3 and TIM3 identifies a potent Treg population that suppresses macrophage functions in colorectal cancer patients. *Clin. Exp. Pharmacol. Physiol.* **45**, 1002–1009 (2018).
18. W. Su, H. Fan, M. Chen, J. Wang, D. Brand, X. He, V. Quesniaux, B. Ryffel, L. Zhu, D. Liang, S. G. Zheng, Induced $CD4^+$ forkhead box protein-positive T cells inhibit mast cell function and established contact hypersensitivity through TGF-β1. *J. Allergy Clin. Immunol.* **130**, 444–452.e447 (2012).
19. Q. Lan, X. Zhou, H. Fan, M. Chen, J. Wang, B. Ryffel, D. Brand, R. Ramalingam, P. R. Kiela, D. A. Horwitz, Z. Liu, S. G. Zheng, Polyclonal $CD4^+Foxp3^+$ Treg cells induce TGFβ-dependent tolerogenic dendritic cells that suppress the murine lupus-like syndrome. *J. Mol. Cell Biol.* **4**, 409–419 (2012).
20. N. Kong, Q. Lan, M. Chen, T. Zheng, W. Su, J. Wang, Z. Yang, R. Park, G. Dagliyan, P. S. Conti, D. Brand, Z. Liu, H. Zou, W. Stohl, S. G. Zheng, Induced T regulatory cells suppress osteoclastogenesis and bone erosion in collagen-induced arthritis better than natural T regulatory cells. *Ann. Rheum. Dis.* **71**, 1567–1572 (2012).
21. L. Danks, N. Komatsu, M. M. Guerrini, S. Sawa, M. Armaka, G. Kollias, T. Nakashima, H. Takayanagi, RANKL expressed on synovial fibroblasts is primarily responsible for bone erosions during joint inflammation. *Ann. Rheum. Dis.* **75**, 1187–1195 (2016).
22. R. E. Simmonds, B. M. Foxwell, Signalling, inflammation and arthritis: NF-κB and its relevance to arthritis and inflammation. *Rheumatology* **47**, 584–590 (2008).
23. W. Sun, R. Qin, R. Qin, R. Wang, D. Ding, Z. Yu, Y. Liu, R. Hong, Z. Cheng, Y. Wang, Sam68 promotes invasion, migration, and proliferation of fibroblast-like synoviocytes by enhancing the NF-κB/P65 pathway in rheumatoid arthritis. *Inflammation* **41**, 1661–1670 (2018).
24. J. Zuo, Q. Yin, Y.-W. Wang, Y. Li, L.-M. Lu, Z.-G. Xiao, G.-D. Wang, J.-J. Luan, Inhibition of NF-κB pathway in fibroblast-like synoviocytes by α-mangostin implicated in protective effects on joints in rats suffering from adjuvant-induced arthritis. *Int. Immunopharmacol.* **56**, 78–89 (2018).
25. P. Li, I. Sanz, R. J. O'Keefe, E. M. Schwarz, NF-κB regulates VCAM-1 expression on fibroblast-like synoviocytes. *J. Immunol.* **164**, 5990–5997 (2000).
26. Y. Zheng, L. Sun, T. Jiang, D. Zhang, D. He, H. Nie, TNFα promotes Th17 cell differentiation through IL-6 and IL-1β produced by monocytes in rheumatoid arthritis. 2014, 385352 (2014).
27. S. Sakaguchi, T. Yamaguchi, T. Nomura, M. Ono, Regulatory T cells and immune tolerance. *Cell* **133**, 775–787 (2008).
28. J. Miao, P. Zhu, Functional defects of Treg cells: New targets in rheumatic diseases, including Ankylosing Spondylitis. *Curr. Rheumatol. Rep.* **20**, 30 (2018).
29. A. M. Gizinski, D. A. Fox, T cell subsets and their role in the pathogenesis of rheumatic disease. *Curr. Opin. Rheumatol.* **26**, 204–210 (2014).
30. F. A. Cooles, J. D. Isaacs, Pathophysiology of rheumatoid arthritis. *Curr. Opin. Rheumatol.* **23**, 233–240 (2011).
31. H. Takayanagi, Osteoimmunology: Shared mechanisms and crosstalk between the immune and bone systems. *Nat. Rev. Immunol.* **7**, 292–304 (2007).
32. N. Kong, Q. Lan, M. Chen, J. Wang, W. Shi, D. A. Horwitz, V. Quesniaux, B. Ryffel, Z. Liu, D. Brand, H. Zou, S. G. Zheng, Antigen-specific transforming growth factor β-induced Treg cells, but not natural Treg cells, ameliorate autoimmune arthritis in mice by shifting the Th17/Treg cell balance from Th17 predominance to Treg cell predominance. *Arthritis Rheum.* **64**, 2548–2558 (2012).
33. M. Tsuji, N. Komatsu, S. Kawamoto, K. Suzuki, O. Kanagawa, T. Honjo, S. Hori, S. Fagarasan, Preferential generation of follicular B helper T cells from $Foxp3^+$ T cells in gut Peyer's patches. *Science* **323**, 1488–1492 (2009).
34. L. Lu, J. Wang, F. Zhang, Y. Chai, D. Brand, X. Wang, D. A. Horwitz, W. Shi, S. G. Zheng, Role of SMAD and non-SMAD signals in the development of Th17 and regulatory T cells. *J. Immunol.* **184**, 4295–4306 (2010).
35. S. G. Zheng, J. D. Gray, K. Ohtsuka, S. Yamagiwa, D. A. Horwitz, Generation ex vivo of TGF-β-producing regulatory T cells from $CD4^+CD25^-$ precursors. *J. Immunol.* **169**, 4183–4189 (2002).
36. A. L. Hernandez, A. Kitz, C. Wu, D. E. Lowther, D. M. Rodriguez, N. Vudattu, S. Deng, K. C. Herold, V. K. Kuchroo, M. Kleinewietfeld, D. A. Hafler, Sodium chloride inhibits the suppressive function of $FOXP3^+$ regulatory T cells. *J. Clin. Invest.* **125**, 4212–4222 (2015).
37. Y. Luo, Y. Xue, J. Wang, J. Dang, Q. Fang, G. Huang, N. Olsen, S. G. Zheng, Negligible effect of sodium chloride on the development and function of TGF-β-induced $CD4^+$ $Foxp3^+$ Regulatory T cells. *Cell Rep.* **26**, 1869–1879.e3 (2019).
38. S. G. Zheng, J. H. Wang, W. Stohl, K. S. Kim, J. D. Gray, D. A. Horwitz, TGF-β requires CTLA-4 early after T cell activation to induce FoxP3 and generate adaptive $CD4^+CD25^+$ regulatory cells. *J. Immunol.* **176**, 3321–3329 (2006).
39. S.-i. Koizumi, H. Ishikawa, Transcriptional regulation of differentiation and functions of effector T Regulatory cells. *Cell* **8**, 989 (2019).
40. A. Denys, G. Clavel, D. Lemeiter, O. Schischmanoff, M.-C. Boissier, L. Semerano, Aortic VCAM-1: An early marker of vascular inflammation in collagen-induced arthritis. *J. Cell. Mol. Med.* **20**, 855–863 (2016).

41. Z. Chen, A. Laurence, Y. Kanno, M. Pacher-Zavisin, B.-M. Zhu, C. Tato, A. Yoshimura, L. Hennighausen, J. J. O'Shea, Selective regulatory function of Socs3 in the formation of IL-17-secreting T cells. *Proc. Natl. Acad. Sci. U.S.A.* **103**, 8137–8142 (2006).
42. W. Xu, Q. Lan, M. Chen, H. Chen, N. Zhu, X. Zhou, J. Wang, H. Fan, C.-S. Yan, J.-L. Kuang, D. Warburton, D. Togbe, B. Ryffel, S.-G. Zheng, W. Shi, Adoptive transfer of induced-Treg cells effectively attenuates murine airway allergic inflammation. *PLOS ONE* **7**, e40314 (2012).
43. K. E. Kim, S. Kim, S. Park, Y. Houh, Y. Yang, S. B. Park, S. Kim, D. Kim, D. Y. Hur, S. Kim, H. J. Park, S. I. Bang, D. Cho, Therapeutic effect of erythroid differentiation regulator 1 (Erdr1) on collagen-induced arthritis in DBA/1J mouse. *Oncotarget* **7**, 76354–76361 (2016).

Acknowledgments
Funding: This work was supported in part by grants from the NIH R01 AR059103, NIH STAR Award, and R61 AR073409 (to S.G.Z.), China National Natural Science Foundation (nos. 81671611 and 81871224 to S.Y.), and Program for Guangdong Introducing Innovative and Entrepreneurial Teams (2016ZT06S252 to F.H.). **Author contributions:** S.Y. and X.Z. performed most of the experiments; analyzed, acquired, and interpreted the data; and drafted the manuscript. J.C. performed most of the experiments analysis and manuscript revision. J.D., R.L., D.Z., H.Z., Y.X., Y.Li., W.W., J.Z., and J.W. performed some experiments. N.O., W.H., Y.P., H.X., B.S., F.H., and Y. Lu analyzed the data and revised the manuscript. S.G.Z. conceived and designed the study and wrote the manuscript. All coauthors approved the final version. **Competing interests:** The authors declare that they have competing interest. **Data and materials availability:** All data needed to evaluate the conclusions in the paper are present in the paper and/or the Supplementary Materials. Additional data related to this paper may be requested from the authors.

Submitted 27 January 2020
Accepted 10 September 2020
Published 28 October 2020
10.1126/sciadv.abb0606

Citation: S. Yang, X. Zhang, J. Chen, J. Dang, R. Liang, D. Zeng, H. Zhang, Y. Xue, Y. Liu, W. Wu, J. Zhao, J. Wang, Y. Pan, H. Xu, B. Sun, F. Huang, Y. Lu, W. Hsueh, N. Olsen, S. G. Zheng, Induced, but not natural, regulatory T cells retain phenotype and function following exposure to inflamed synovial fibroblasts. *Sci. Adv.* **6**, eabb0606 (2020).